Journal of Energy and Power Engineering 18 (2024) 46-58
doi: 10.17265/1934-8975/2024.02.002

Comprehensive Molten Salt Storage Shell and Support Design and Analysis IV: A Complete 700°C Thermal-Structural Interaction Finite Element Analysis of an 80 Foot Diameter and 46 Foot High MS Storage Shell Including Structural, Conductive and Convective Thermal Stress Analysis

Nathan Loyd and Samaan Ladkany
Howard Hughes College of Engineering, University of Nevada, Las Vegas, NV 89154, USA

Abstract: In this paper a finite element structural analysis model—using COMSOL—of a large molten salt container, 80 foot in diameter and 46 feet high that includes a four-foot elliptic shell roof, is presented for a futuristic 700 ℃ design, which uses a highly stable chloride salt called SS700 (SaltStream 700) that improves the efficiency of the tank when compared to the traditional 565 ℃. The resulting FEA (finite element analysis) computed the stresses induced in the tank, which includes the stresses that are due to the loading and due to the thermal expansion of the tank. A stress FEA model was developed using COMSOL Version 5.4 in order to determine the full thermal stress and total stress distribution of the 700 ℃ Cylindrical MS Storage Tank, as well as corresponding temperature distributions, which can be used to compare with the theoretical analysis and verify the final design.

Key words: Molten salts, storage tank design, solar energy, shell theory, FEA.

1. Introduction

This paper is a follow up to our previous three papers, “Molten Salt History, Types, Thermodynamic and Physical Properties, and Cost” (2018), “565℃ Molten Salt Solar Energy Storage Design, Corrosion, and Insulation” (2018) and “Worldwide Molten Salt Technology Developments in Energy Production and Storage” (2018), all in the *Journal of Energy and Power Engineering*. This paper is the final paper in a four-paper follow up series in MS solar energy storage that gives a complete and comprehensive analysis and design of the storage shells [1-3].

Molten solar salts have considerable capacities for heat storage, which makes them effective at storing excess solar energy and other types of energy, such as nuclear. Large insulted tanks provide a closed system for these molten salts to be properly contained [4].

In this paper a finite element structural analysis model—using COMSOL—of a large molten salt container, 80 foot in diameter and 46 feet high that includes a four-foot elliptic shell roof, is presented for a futuristic 700 ℃ design, which uses a highly stable chloride salt called SS700 (SaltStream 700) that improves the efficiency of the tank when compared to the traditional 565 ℃. The resulting FEA (finite element analysis) computed the stresses induced in the

Corresponding author: Samaan Ladkany, PhD, professor, research fields: civil structural engineering, shells structures, steel structures.

tank, which includes the stresses that are due to the loading and due to the thermal expansion of the tank [4]. This stress FEA is a follow up to the heat transfer FEA performed by Loyd et al. [5], as well as a follow up to the structural design provided by Loyd et al. [6].

2. FEM Structural Analysis

A stress FEA was developed using COMSOL Version 5.4 in order to determine the full thermal stress and total stress distribution of the 700 ℃ Cylindrical MS Storage Tank, as well as corresponding temperature distributions [4]. However, the structural design of the tank does allow for free expansion, meaning that the tank should not have any thermal stresses. Any provided definitions are from Version 5.4 of the COMSOL Multiphysics Reference Manual [7].

This FEM (finite element model) requires various inputs in order to carry out the FEA in COMSOL. As explained in detail in Loyd et al. [5], the first step is to import the 2D axisymmetric model of the shell into COMSOL, in this case an AutoCAD drawing of the 700 ℃ Cylindrical MS Storage Tank. Once the model is imported, it is refined by adding material properties and defining the mesh. After this, loading and heat transfer conditions are assigned to the model and a time study is defined, with the time study correlating to the 50-year lifespan of the model [4, 5].

2.1 FEM Model Inputs in COMSOL

Modeling the 700 ℃ Cylindrical MS Storage Tank into COMSOL required various considerations. Loyd [4] and Loyd et al. [5] detail these considerations as such.

A model of the 700 ℃ Cylindrical MS Storage Tank must be created in COMSOL in order to perform the FEA. For an axisymmetric analysis, this is accomplished by importing an AutoCAD DXF file of the 2D tank outline into COMSOL, with the resulting outline in COMSOL shown in Fig. 1. With this outline, COMSOL then constructs the tank components. Once the tank model was imported into COMSOL, a rectangular section below the prestressed concrete slab was added for the 60 foot wide section to include the extra depth of sand in the FEM. Another rectangle was also included for the portion of the ground below that exists to the side of prestressed slab, which is needed for the 500 foot by 500 foot and 1,000 foot by 1,000 foot configurations.

The number of mesh elements and their properties used in the FEM under three different scenarios are detailed in Table 1. The ground section under the tank was limited to 500 feet by 60 feet in the initial analysis. This analysis made it apparent that expanding this section was needed in order to accommodate the full heat transfer effects, which was expanded to 500 feet by 500 feet. After this, the below ground section was expanded to 1,000 feet by 1,000 feet to see if the heat transfer effects would stabilize or not, and they did stabilize.

Table 1 presents the geometric properties of the model mesh, which is further explained in Refs. [4, 5].

Based on Table 1, the number of elements in each of these configurations is roughly the same. In the 500 foot by 60 foot below ground configuration, there are 46,903 triangular elements, 8,299 edge elements, and 61 vertex elements. In the 500 foot by 500 foot below ground configuration, there are 47,381 triangular elements, 8,343 edge elements, and 63 vertex elements. In the 1,000 foot by 1,000 foot below ground configuration, there are 47,261 triangular elements, 8,314 edge elements, and 63 vertex elements. The minimum element quality is 0.007676 for the 500 foot by 60 foot configuration as well as the 500 foot by 500 foot configuration, and 0.8987 for the 1,000 foot by 1,000 foot configuration. The average element quality is 0.9086 for the 500 foot by 60 foot configuration, 0.9094 for the 500 foot by 500 foot configuration, and 0.8987 for the 1,000 foot by 1,000 foot configuration. The maximum element size in inches for these configurations is 442 for the 500 foot by 60 foot configuration as well as the 500 foot by 500 foot configuration, and 844 for the 1,000 foot by 1,000 foot configuration. The maximum element size in inches for these configurations is 1.98 for the 500 foot by 60 foot configuration as well as the 500 foot by 500 foot configuration, and 3.78 for the 1,000 foot by 1,000 foot configuration. The curvature factor, which limits how the elements along curved surfaces are sized, is set to its default setting of 0.3 for all simulations. The growth factor, which dictates how neighboring elements are sized relative to each other, is also set to its default setting of 1.3 for all simulations. All of this information indicates that increasing the size of the below ground section of the FEM will result in size increases of the elements since the number of elements for each configuration only varies slightly [7].

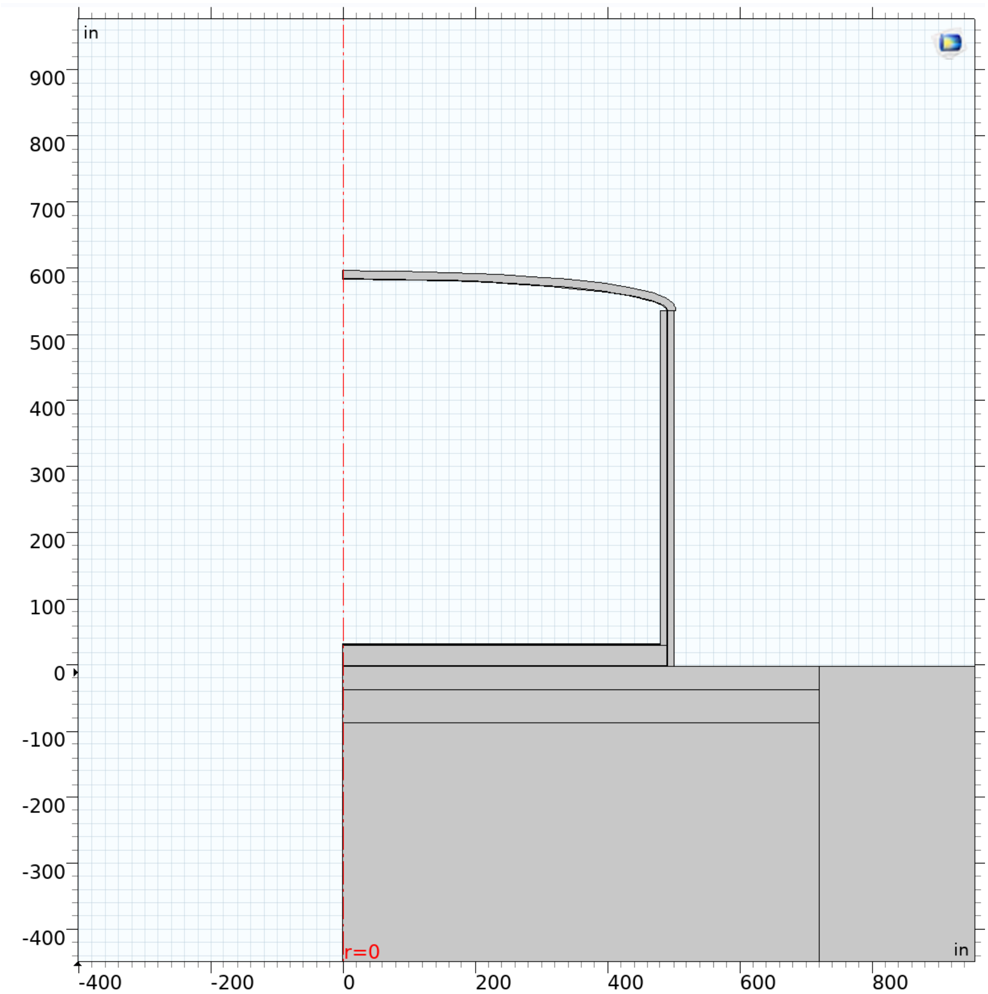

Fig. 1 700 ℃ Cylindrical MS Storage Tank outline and surrounding components [4, 5].

Table 1 Element properties of the various FEM model configurations [4, 5].

Ground configuration	500′ × 60′	500′ SQ	1,000′ SQ
Triangular elements	46,903	47,381	47,261
Edge elements	8,299	8,343	8,314
Vertex elements	61	63	63
Min. element quality	0.007676	0.007676	0.007255
Avg. element quality	0.9086	0.9094	0.8987
Max. element size (in)	442	442	844
Min. element size (in)	1.98	1.98	3.78
Curvature factor	0.3	0.3	0.3
Max. growth rate	1.3	1.3	1.3

This further details the use of triangular elements in COMSOL rather than the conventional use of rectangular elements [4, 5].

Triangular elements were used since they fully fit without discontinuities to the varying geometry of the tank, the hybrid wall structure of the cylinder, and the various geometries presented in this research of the top roof shells. The triangular elements provide natural transition at corners and between different materials of the structure and the foundation. It is important to note that COMSOL only allows triangular elements in soils insulators because soils are not elastic, even if fully compacted as recommended under the shell bottom plate. Also, triangular elements are preferred for heat transfer analysis, therefore a full and smooth transition between the bottom plate and the sand layers and the rest of the foundation structure under the 700 ℃ Cylindrical MS Storage Tank.

Loyd [4] and Loyd et al. [5] detail the design considerations of the tank in further detail:

The ambient air temperature for the FEM is 20 ℃, which means all tank components except the most inner layer of the tank are set to this temperature. For the inner boundaries in contact with the salt, the initial temperatures are set to the salt temperature of 700 ℃. As for all components that are below ground, the starting temperature is set to the ambient soil temperature of 15 ℃. As for the boundary loads along the stainless steel, which is due to the hydrostatic pressure of the molten salt, the unit weight is set to 19,908 N/m^3.

The mesh for sections around the 700 ℃ Cylindrical MS Storage Tank are shown in Fig. 2. A close up of the mesh around the tank roof is shown in Fig. 3. A close up of the mesh around the junction of the base of the tank and the shell wall is shown in Fig. 4. The full mesh used for the below ground section of the tank in the 1,000 foot by 1,000 foot configuration is shown in Fig. 5. It is apparent that the elements for most of the insulating and structural layers of the tank are smaller in size, which makes sense because of the relatively thin layer thicknesses with both the stainless and carbon steel layers. The larger mesh elements correspond to the below ground mesh elements due to the larger material sizes comprising this section.

The material properties of the 700 ℃ Cylindrical MS Storage Tank used in COMSOL for the FEA are shown in Fig. 6. The six materials used include stainless steel, carbon steel, insulating firebrick, ceramic insulation, silica sand, and concrete. Density, Young's modulus, Poisson's ratio, thermal conductivity, heat capacity, and the coefficient of thermal expansion are among the important properties used in defining the model.

2.2 Axisymmetric FEA

Using an axisymmetric FEA provided for a more efficient analysis compared to traditional 3D FEA analysis because of the model symmetry. This symmetry occurs because the 3D model is constructed by the revolution of a 2D shell, allowing for a 2D analysis as detailed by loyd et al. [4, 5] and Cook [8].

The term "3D solid" is used to mean a three-dimensional solid that is unrestricted as to shape, loading, material properties, and boundary conditions. A consequence of this generality is that all six possible stresses (three normal and three shear) must be taken into account. Also, the displacement field involves all three possible components: *u*, *v*, and *w*. Typical finite elements for 3D solids are tetrahedra and hexahedra with three translational d.o.f. per node.

Problems of beam bending, plane stress, plates, and so on, can all be regarded as special cases of a 3D solid. Why then not simplify FE analysis by using 3D elements to model everything? In fact, this would not be a simplification. 3D models are the hardest to prepare, the most tedious to check for errors, and the most demanding of computer resources. Also, some 3D elements would become quite elongated in modeling beams, plates, and shells; this invites locking behavior and ill-conditioning.

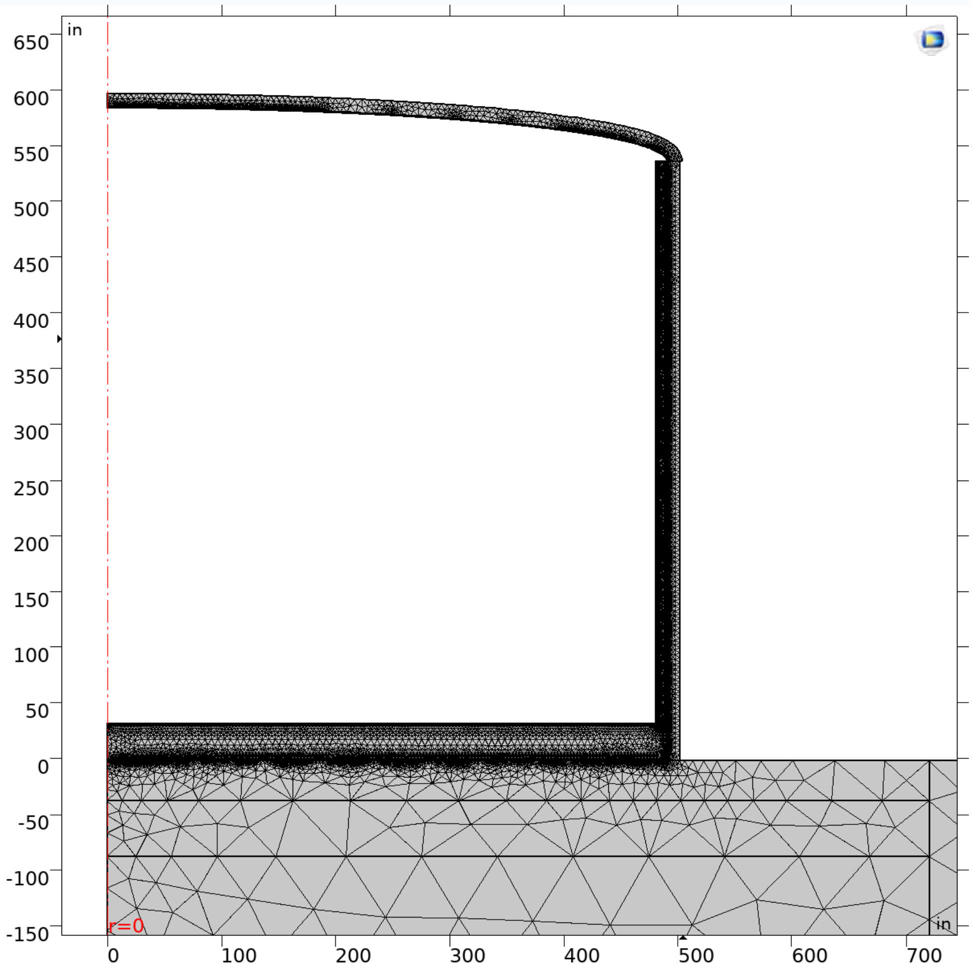

Fig. 2 Close up of 700 ℃ Cylindrical MS Storage Tank mesh [4, 5].

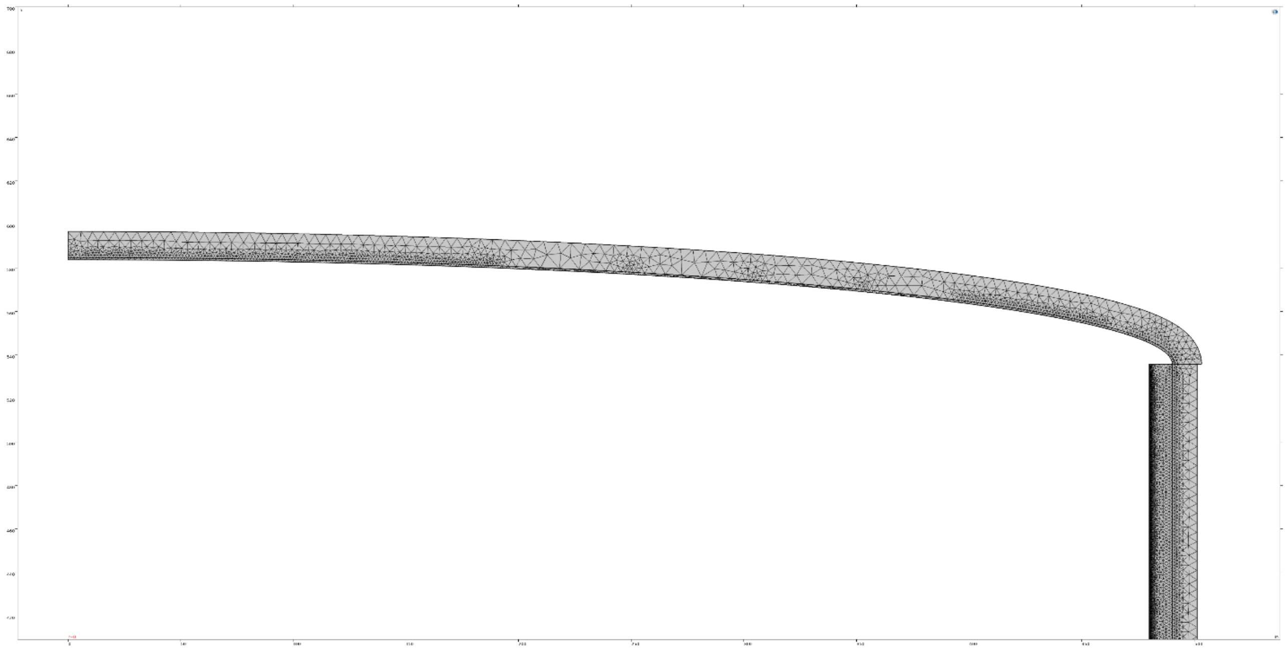

Fig. 3 Close up of 700 ℃ Cylindrical MS Storage Tank roof mesh [4, 5].

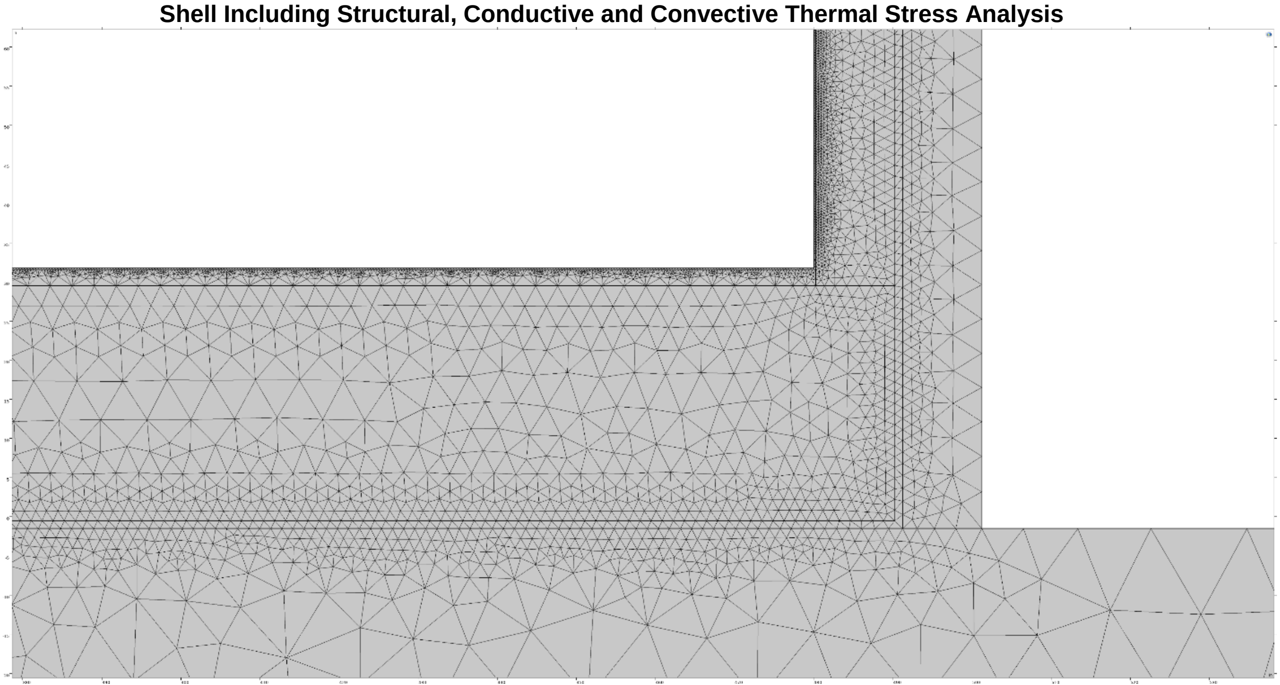

Fig. 4 Close up of 700 ℃ Cylindrical MS Storage Tank mesh at the shell wall and base junction [4, 5].

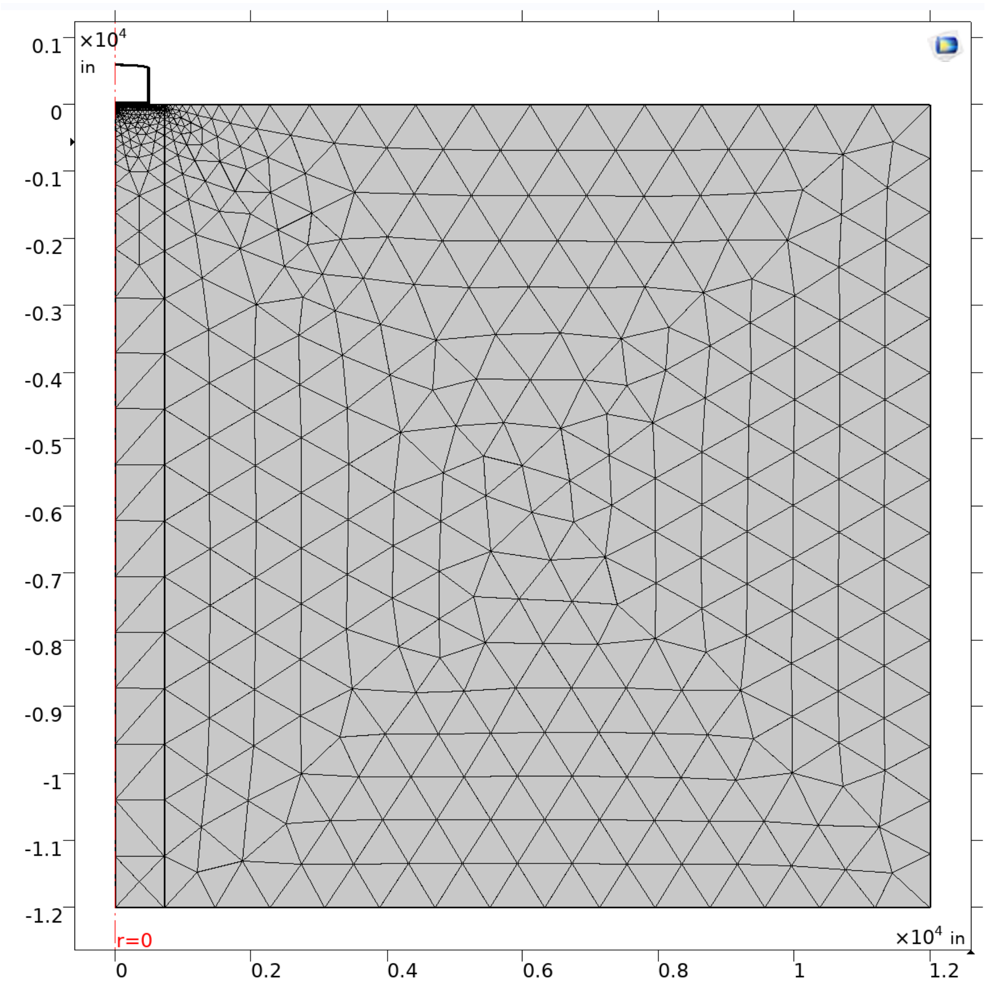

Fig. 5 Below ground mesh of 700 ℃ Cylindrical MS Storage Tank [4, 5].

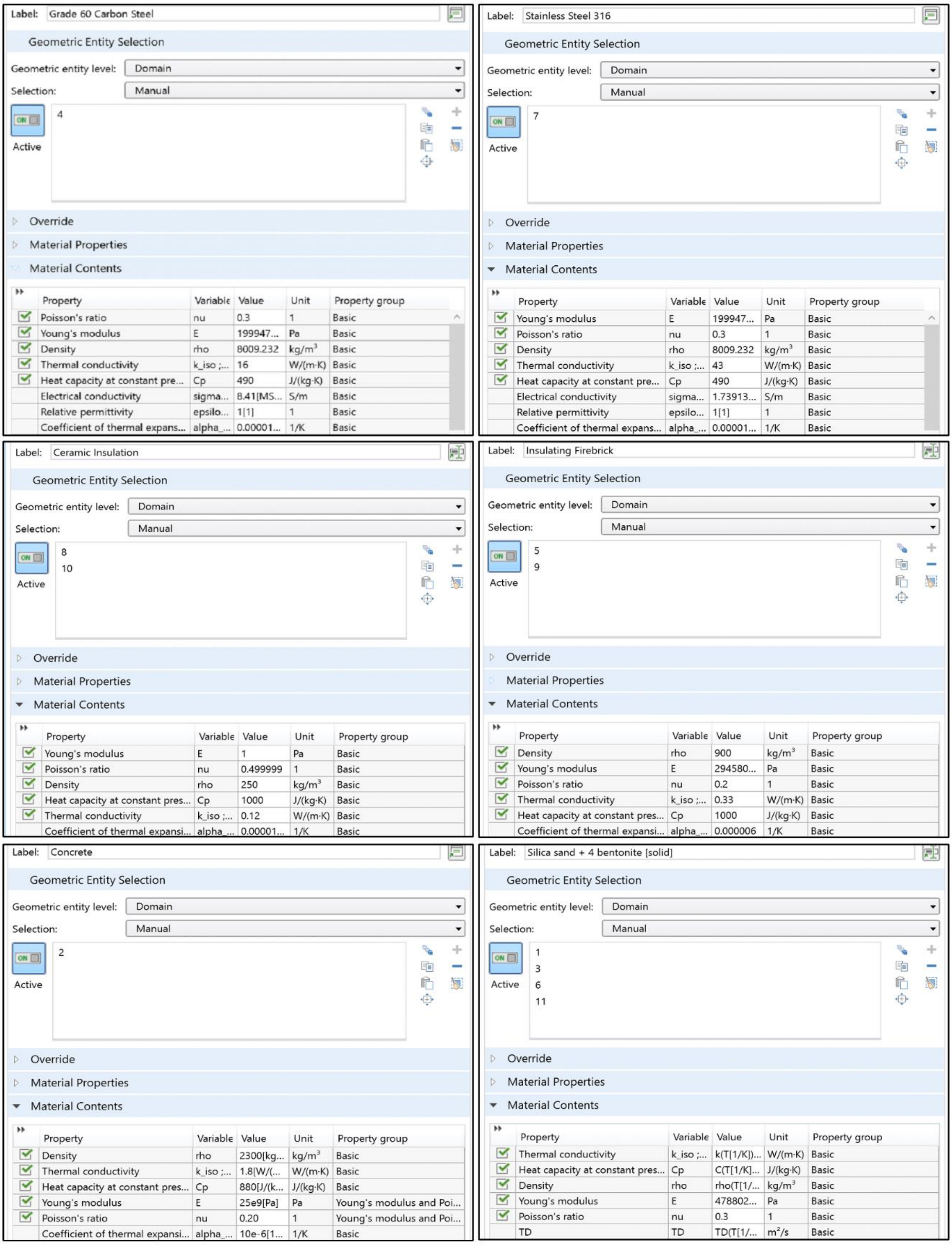

Fig. 6 700 ℃ Cylindrical MS Storage Tank material properties used in COMSOL [4, 5].

A solid of revolution, also called an axisymmetric solid, is generated by revolving a plane figure about an axis in the plane. Common examples include a hose nozzle and a light bulb, although the light bulb has a very thin wall and would be properly classed as a shell of revolution for stress analysis purposes. Loads and supports may or may not have axial symmetry. Initially, we will consider the case where geometry, elastic properties, loads, and supports are all axisymmetric. Consequently, nothing varies with the circumferential coordinate θ, material points displace only radially and axially, and shear stresses $\tau_{r\theta}$ and $\tau_{\theta z}$, are both zero. Thus the analysis problem is mathematically two-dimensional. Axisymmetric finite elements are often pictured as plane triangles or quadrilaterals, but these plane shapes are actually cross sections of annular elements, and what appear to be nodal points are actually nodal circles.

A further discussion on how the effects of the above information affects the resulting analysis [4, 5, 8]:

Because of the information above, it is apparent that an axisymmetric model has four degrees of freedom versus six in a traditional 3D model. This reality is reflected in Eqs. (1)-(3). Eq. (1) is the general strain matrix for a node, which can be used in both axisymmetric and traditional 3D models. For traditional 3D models, matrix **B** is a 6 $\times 3n$ matrix, with n representing the number of nodes in the model, and vector d is a $3n \times 1$ vector, which leads to vector ε being a 6 $\times$ 1 vector. As for an axisymmetric model, **B** is a 4 $\times 2n$ matrix and d is a $2n \times 1$ vector, which means ε is a reduced 4 $\times$ 1 vector in an axisymmetric model. Eq. (2) details how the stiffness matrix is calculated in a traditional 3D model with n nodes. As mentioned earlier, the **B** matrix in a traditional 3D model is a 6 $\times$ $3n$ matrix, which means that the **E** matrix must be a 6 $\times$ 6 matrix for the matrix math to occur, which results in the **K** matrix being a $3n \times 3n$ matrix. Eq. (3) details how the stiffness matrix is calculated in an axisymmetric model with n nodes. As mentioned earlier, the **B** matrix in an axisymmetric model is a 4 $\times$ $2n$ matrix, which means that the **E** matrix must be a 4 $\times$ 4 matrix for the matrix math to occur, which results in the **K** matrix being a reduced $2n \times 2n$ matrix.

$$\boldsymbol{\varepsilon} = \boldsymbol{B}\ \boldsymbol{d} \tag{1}$$

$$\boldsymbol{K} = \int\int\int \boldsymbol{B}^T\ \boldsymbol{E}\ \boldsymbol{B}\ dx\ dy\ dz \tag{2}$$

$$\boldsymbol{K} = \int\int\int \boldsymbol{B}^T\ \boldsymbol{E}\ \boldsymbol{B}\ dr\ d\theta\ dz \tag{3}$$

Further detail on the boundary effects of the analysis from Loyd et al. [4, 5] and Cook [8] is provided below:

To prevent singularity of *K*, boundary conditions on a 3D solid must suppress six rigid-body motions: translation along, and rotation about, each of the three coordinate axes. In a solid of revolution with axisymmetric deformations, translation *w* along the *z* axis is the only possible rigid-body motion. Accordingly, K will be nonsingular if *w* is prescribed at only one node (or, stated more properly, around one nodal circle).

An axisymmetric radial component of load is statically equivalent to zero, but this does not mean that it can be discarded from the load vector. It still produces deformation and stress. Over the circumference, a radial line load of *q* units of force per unit of (circumferential) length is regarded as contributing a radial force $2\pi rq$ of units to the load vector, where *r* is the radius at which *q* acts. Likewise, a moment of M N ·m per unit of (circumferential) length is statically equivalent to zero but is regarded as applying a moment about the *e* direction of $2\pi rM$ N ·m. Similar remarks can be made for the radial body force load associated with spinning about the *z* axis.

An unrestrained body that is homogeneous and either isotropic or rectilinearly orthotropic is unstressed by temperature change if the temperature field is either constant or linear in Cartesian coordinates *xyz*. An unrestrained solid of revolution that is either isotropic or cylindrically orthotropic is not unstressed by a temperature field that is linear in radius *r* of cylindrical coordinates. The solid of revolution would remain stress-free if the temperature field is either constant or a linear function of axial coordinate *z* only.

Although a plane FE model and the cross section of an axisymmetric FE model look alike, and each uses the same pattern of nodal d.o.f., it is physically meaningless to couple them together. Physically, such a connection would not produce axisymmetric deformations in the solid of revolution. If this kind of connection is actually intended, it will usually be necessary to model the solid of revolution by 3D elements.

2.3 FEM Structural Analysis Equations in COMSOL

The linear elastic structural analysis of the structure is conducted using the set of equation that are shown in Fig. 7. This linear elastic analysis is performed using energy methods to compute the stress-strain relationships of the model [4, 5, 7].

Eq. (4) details the Von Mises stress equation, which are the stresses that are computed by the FEA. These stresses represent a 3D state of stress which includes hoop stresses in the circumferential directions. For the equations shown in Fig. 7, the acceleration is zero since there is no motion in the structure. Eq. (5) details Fourier Series loading, which is what would need to be used in COMSOL for computing a seismic analysis. The displacement equations would follow the same format, in that all of these Fourier series equations will have sine and cosine terms, with *n* representing the harmonic number in the sequence, with q_{cn} and q_{sn} represent the initial magnitudes of the series [4, 5, 8].

$$\sigma = \sqrt{\frac{1}{2}[(\sigma_1-\sigma_2)^2+(\sigma_1-\sigma_3)^2+(\sigma_2-\sigma_3)^2]} \qquad (4)$$

$$q = \sum_{n=0}^{\infty}(q_{cn}\cos n\theta) + \sum_{n=0}^{\infty}(q_{sn}\sin n\theta) \qquad (5)$$

One last important consideration for this analysis is the time study, which is conducted over the 50-year lifespan of the structure. This results in the use of a dependent time study, which performs an FEA of the structure at one year intervals until the end of the lifespan. This is performed for both the thermal and stress analysis [4, 5].

$$\rho\frac{\partial^2 \mathbf{u}}{\partial t^2} = \nabla\cdot S + \mathbf{F}_V$$

$$S = S_{ad} + \mathbf{C}:\epsilon_{el}, \quad \epsilon_{el} = \epsilon - \epsilon_{inel}$$

$$\epsilon_{inel} = \epsilon_0 + \epsilon_{ext} + \epsilon_{th} + \epsilon_{hs} + \epsilon_{pl} + \epsilon_{cr} + \epsilon_{vp}$$

$$S_{ad} = S_0 + S_{ext} + S_q$$

$$\epsilon = \frac{1}{2}\left[(\nabla\mathbf{u})^T + \nabla\mathbf{u}\right]$$

$$\mathbf{C} = \mathbf{C}(E,\nu)$$

Fig. 7 Structural analysis equations for linearly elastic materials [4, 7].

3. FEM Stress Analysis Results

Computation for the FEA can be begun once the inputs have been incorporated into the model. The resulting analysis determines the temperature and stress distributions of the model, which are included in a full report generated by COMSOL. While the time study covers the entirety of the 50 year lifespan, the results presented in the paper are focused on the stress effects at the 50-year mark. [4]

3.1 FEM Stress Results from COMSOL

To start the FEA on COMSOL, the first step was to verify thermal expansion effects. Fig. 8 shows the resulting stresses due to thermal effects in the tank.

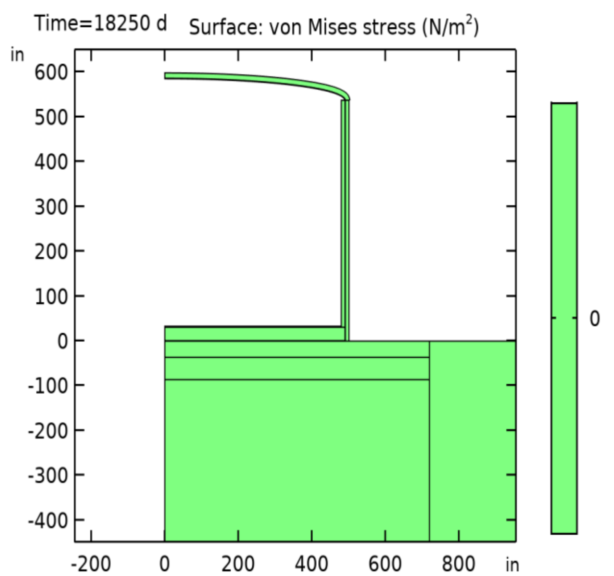

Fig. 8 Thermal stresses for the 700 ℃ Cylindrical MS Storage Tank [4].

As expected, Fig. 8 shows that there are no thermal stresses for the 700 ℃ Cylindrical MS Storage Tank. This is because the tank was designed for free thermal expansion in the shell wall with a gap the was calculated so that the shell wall components would expand into each other at 700 ℃. The tank also sits on granular sand that allows for the bottom to thermally expand freely with damage to the bottom of the tank [4].

The total stress distribution of the axisymmetric 2D shell for the 700 ℃ Cylindrical MS Storage Tank is shown in Fig. 9, while Fig. 10 shows the full 3D view of the shell stress distribution. Shown in Fig. 11 is the stress distribution at the intersection of the shell wall and base for the 700 ℃ Cylindrical MS Storage Tank [4].

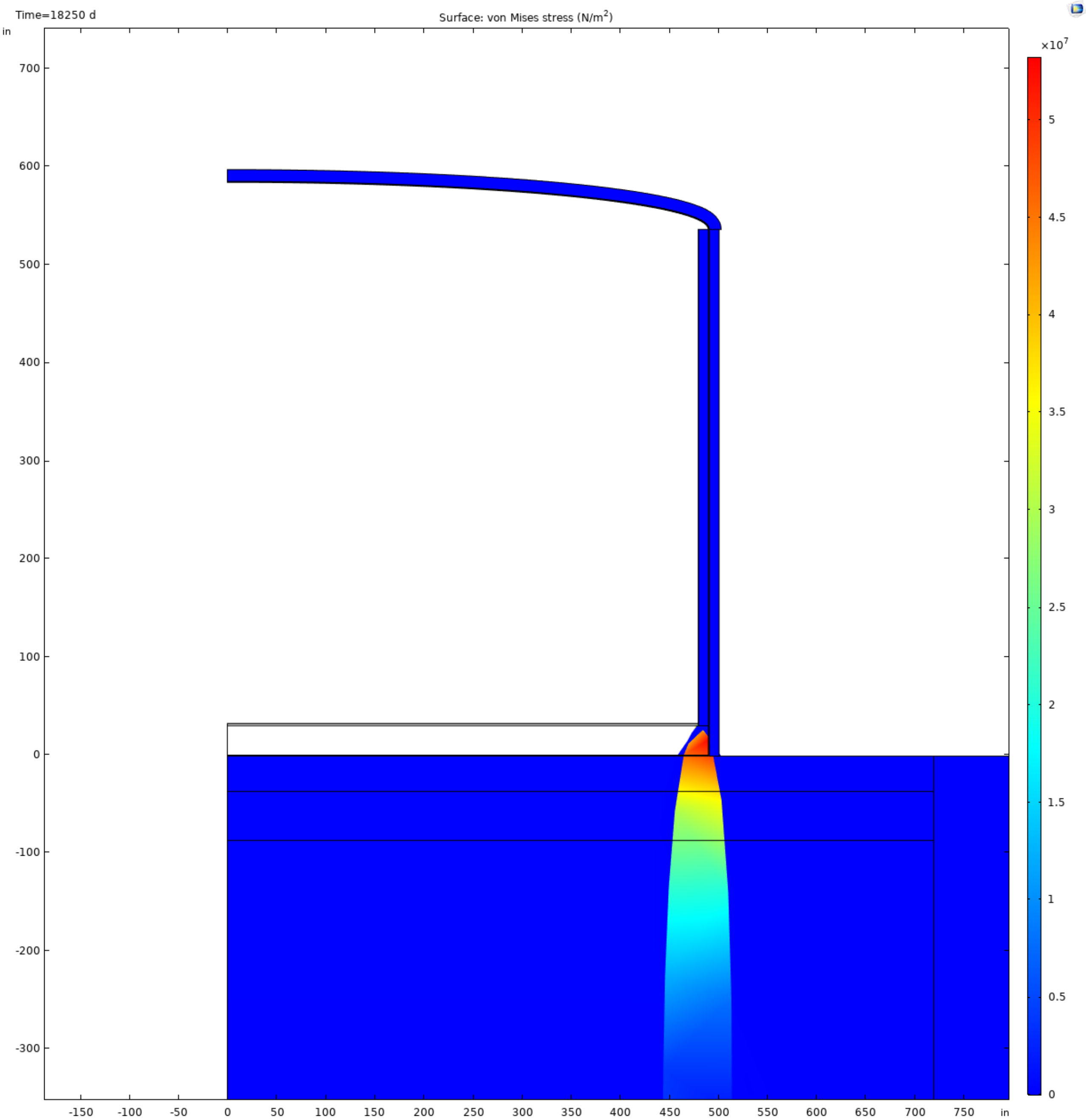

Fig. 9 Axisymmetric total stress distribution in Pascals of the 700 ℃ Cylindrical MS Storage Tank [4].

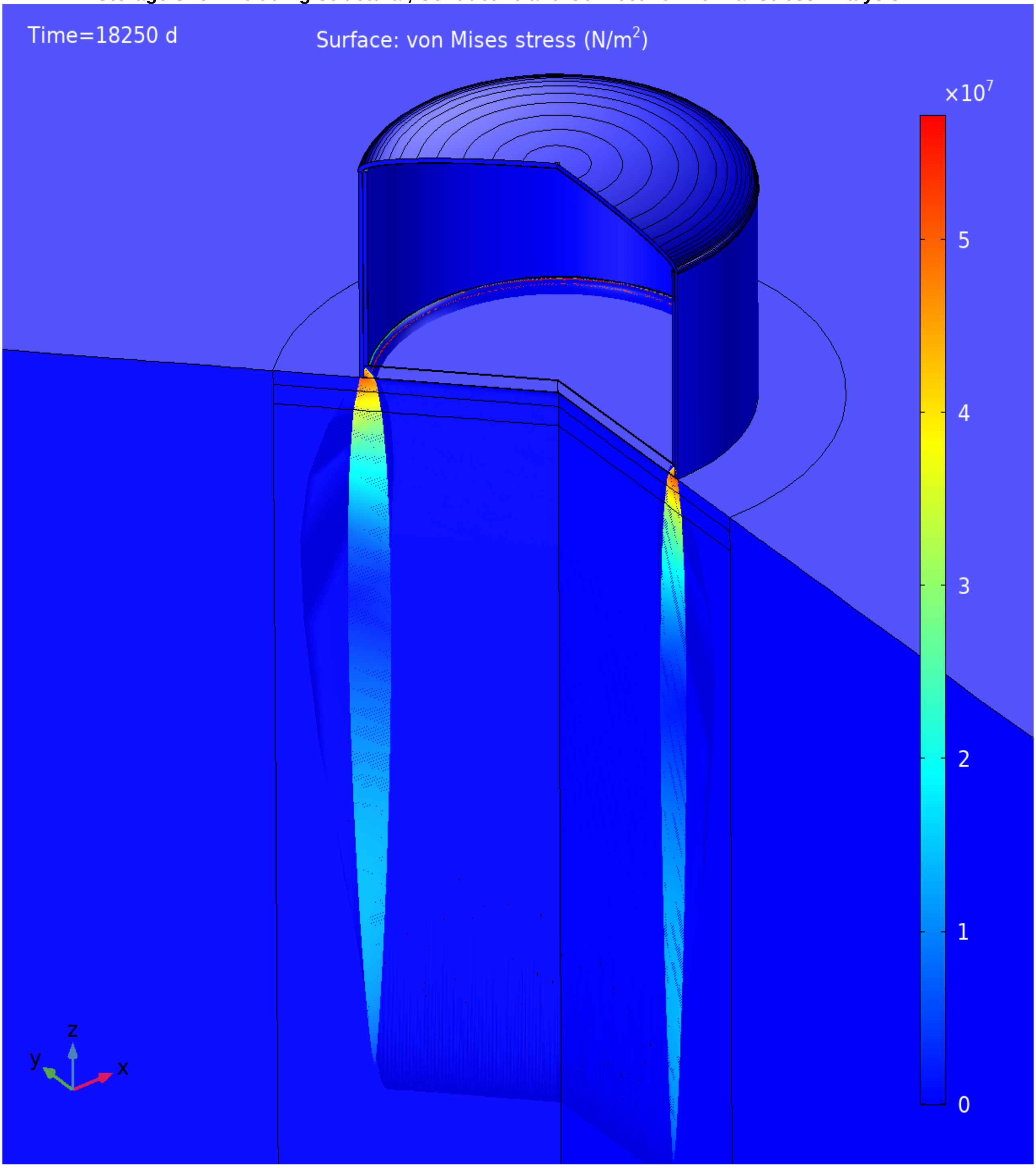

Fig. 10 3D total stress distribution in Pascals of the 700 ℃ Cylindrical MS Storage Tank [4].

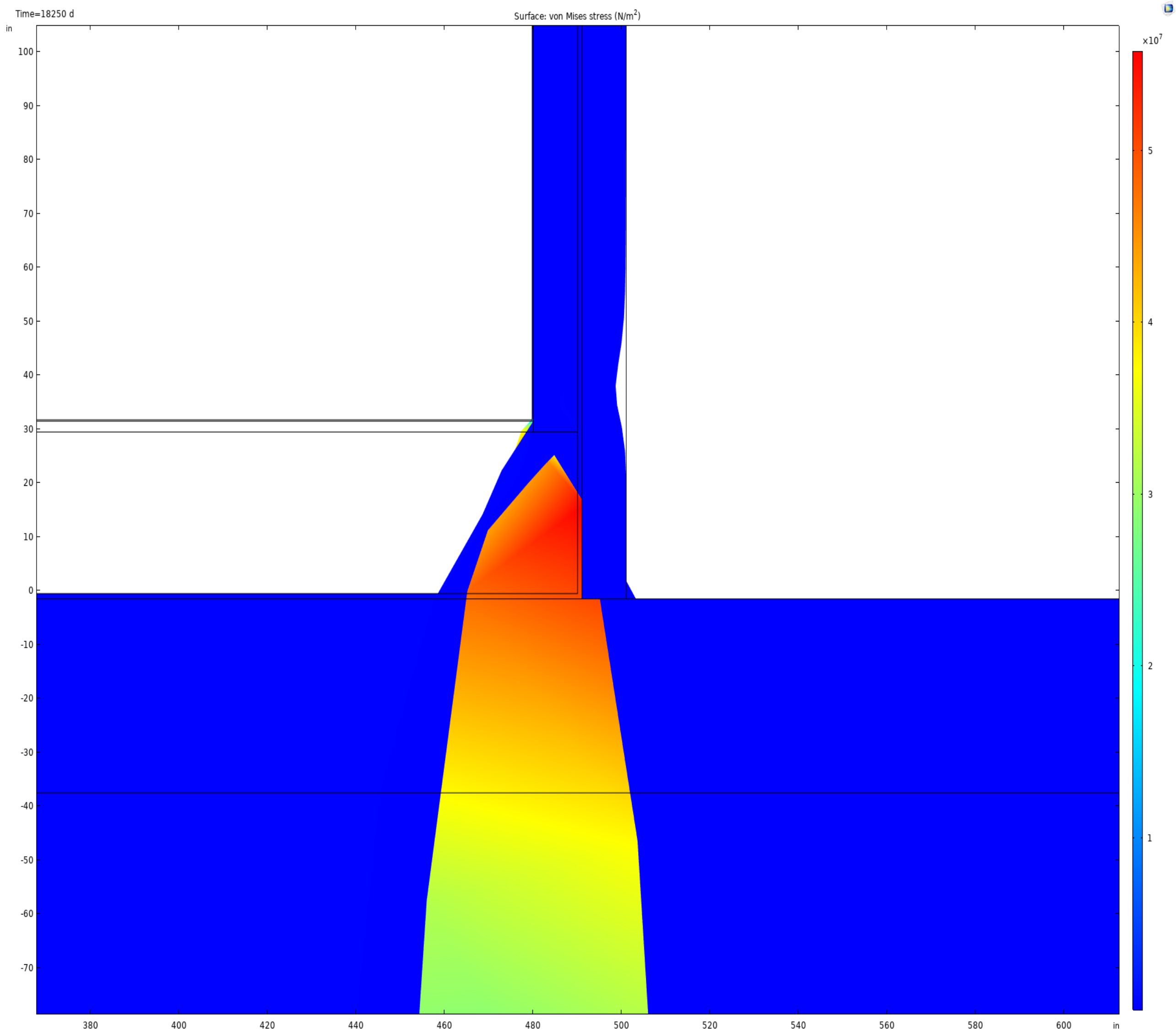

Fig. 11 Axisymmetric total stress distribution in Pascals of the 700 ℃ Cylindrical MS Storage Tank at the junction of the shell wall and the base of the tank [4].

With information shown in these figures, the maximum stress in the carbon steel shell wall occurs at the intersection with the ground firebrick layer, which results in a stress is approximately 60 MPa, or 8,700 pounds psi (per square inch). Loyd [4] further expands on how the stresses develop around the intersection of the shell wall and bottom of the tank:

Stress exists primarily in the region where the side carbon steel wall, the bottom carbon steel plate, and bottom firebrick layer meet, with some stress developing in the soil and concrete slab directly below the shell wall. This would make sense since the structural design focused on making sure that the structural carbon steel would be able to take all of the loading with an allowable stress of 21,600 psi. This was done to ensure that failures in the stainless steel and/or firebrick insulation would not result in structural failure in the carbon steel. As such, having these layers included in the FEM would result in lower stresses along the side wall. In addition, there are no stresses in the roof since it does not have any applied loading on it. Table 2 shows the FEM stress values in the shell wall at various points in the wall at the top and bottom of the wall.

Table 2 FEM shell wall stresses in pounds psi at the top and bottom of the wall [4].

Interval at given shell location	Top	Bottom
Inner edge of the stainless steel	0	1,555
Stainless steel and firebrick junction	0	512
Firebrick and carbon steel junction	0	323
Outer edge of the carbon steel	0	796

Based on Table 2, the results show at the top there is no loading, which makes sense since that is also where the top of the molten salt exists. At the tank bottom, which is measured at the same level as the bottom of the salt, the stresses are relatively low due to the composite nature of the tank. In addition, these stresses are lower than the maximum stress because these stresses are measured above the stress bubble that is present in the junction between the carbon steel shell, carbon steel plate, and the ground firebrick insulation.

4. Conclusions

The results of the stress FEA in COMSOL determined that there are no thermal stresses in the structure as expected. However, the temperature distribution reveals higher than expected temperatures in the model, which can be explained by the fact that the manual heat transfer analysis treated the ground as a semi-infinite material in the analysis [4, 5].

As for the stresses in the carbon steel, the largest stress is present near the junction between the carbon steel shell wall, carbon steel shell plate, and ground firebrick, and is about 40% of the allowable stress of 21,600 ksi for the carbon steel. The other stresses are relatively small due to the redundancy of the structural design, which sees the stainless steel, side firebrick, and carbon steel in the shell wall all taking stresses. This is despite the fact that the shell was designed with the intention that the structural carbon steel be able to take the full loading on its own should there be any failure [4].

Acknowledgments

Our funding for this research came from the ONR (Office of Naval Research). Further support has also come from the University of Nevada, Las Vegas, the Howard Hughes College of Engineering, and the Department of Civil and Environmental Engineering and Construction.

References

[1] Ladkany, S., Culbreth, W., and Loyd, N. 2018. "Molten Salt History, Types, Thermodynamic and Physical Properties, and Cost." *Journal of Energy and Power Engineering* 12 (11): 507-16.

[2] Ladkany, S., Culbreth, W., and Loyd, N. 2018. "565°C Molten Salt Solar Energy Storage Design, Corrosion, and Insulation." *Journal of Energy and Power Engineering* 12 (11): 571-32.

[3] Ladkany, S., Culbreth, W., and Loyd, N. 2018. "Worldwide Molten Salt Technology Developments in Energy Production and Storage." *Journal of Energy and Power Engineering* 12 (11): 533-44.

[4] Loyd, N. 2020. "Alternate Novel Thermal Structure Interaction Designs of Molten Salt Shell Structures at High Temperatures Ranging from 565 ℃ to 700 ℃." PhD thesis, University of Nevada.

[5] Loyd, N., Ladkany, S., and Culbreth, W. 2022. "A Conductive and Convective Theoretical Heat Transfer Analysis for Molten Salt Cylindrical Shells at 565 ℃ and 700°C." *Journal of Energy and Power Engineering* 12: 554.

[6] Loyd, N., Ladkany, S., and Culbreth, W. 2024. "A Complete 700 ℃ Thermal-Structural Interaction Design Using Theoretical Analysis of an 80 Foot Diameter and 46 Foot High MS Storage Shell Including Structural, Conductive and Convective Thermal Stress Analysis." *Journal of Energy and Power Engineering.* (in press)

[7] COMSOL, Inc. 2018. *COMSOL Multiphysics Reference Manual* (version 5.4). www.comsol.com.

[8] Cook, R. 1995. *Finite Element Modeling for Stress Analysis.* New York: John Wiley & Sons.